

Accepted Manuscript

The Immunomodulation Potential of the Synthetic Derivatives of Benzothiazoles: Implications in Immune System Disorders through *in vitro* and *in silico* Studies

Khalid Mohammed Khan, Mohammad A. Mesaik, Omer M. Abdalla, Fazal Rahim, Samreen Soomro, Sobia A. Halim, Ghulam Mustafa, Nida Ambreen, Ahmad Shukralla Khalid, Muhammad Taha, Shahnaz Perveen, Muhammad Tanveer Alam, Abdul Hameed, Zaheer Ul-Haq, Hayat Ullah, Zia Ur Rehman, Rafat Ali Siddiqui, Wolfgang Voelter

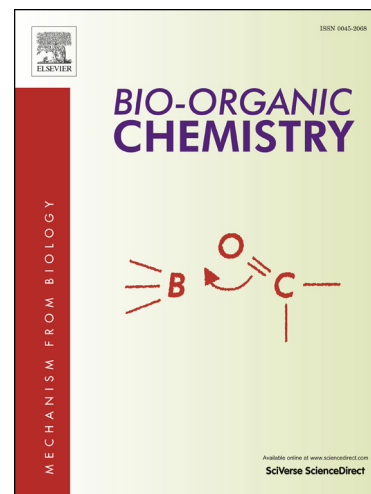
PII: S0045-2068(15)30035-3
DOI: <http://dx.doi.org/10.1016/j.bioorg.2015.11.004>
Reference: YBIOO 1858

To appear in: *Bioorganic Chemistry*

Received Date: 18 September 2015
Revised Date: 12 November 2015
Accepted Date: 17 November 2015

Please cite this article as: K.M. Khan, M.A. Mesaik, O.M. Abdalla, F. Rahim, S. Soomro, S.A. Halim, G. Mustafa, N. Ambreen, A.S. Khalid, M. Taha, S. Perveen, M.T. Alam, A. Hameed, Z. Ul-Haq, H. Ullah, Z.U. Rehman, R.A. Siddiqui, W. Voelter, The Immunomodulation Potential of the Synthetic Derivatives of Benzothiazoles: Implications in Immune System Disorders through *in vitro* and *in silico* Studies, *Bioorganic Chemistry* (2015), doi: <http://dx.doi.org/10.1016/j.bioorg.2015.11.004>

This is a PDF file of an unedited manuscript that has been accepted for publication. As a service to our customers we are providing this early version of the manuscript. The manuscript will undergo copyediting, typesetting, and review of the resulting proof before it is published in its final form. Please note that during the production process errors may be discovered which could affect the content, and all legal disclaimers that apply to the journal pertain.



The Immunomodulation Potential of the Synthetic Derivatives of Benzothiazoles: Implications in Immune System Disorders through *in vitro* and *in silico* Studies

Khalid Mohammed Khan^{a*}, Mohammad A. Mesaik^{b,c*}, Omer M. Abdalla^c, Fazal Rahim^{a,d}, Samreen Soomro^c, Sobia A. Halim^c, Ghulam Mustafa^{c,e}, Nida Ambreen^a, Ahmad Shukralla Khalid^c, Muhammad Taha^a, Shahnaz Perveen^f, Muhammad Tanveer Alam^a, Abdul Hameed^a, Zaheer Ul-Haq^{c,e}, Hayat Ullah^d, Zia Ur Rehman^d, Rafat Ali Siddiqui^g and Wolfgang Voelter^h

^aH. E. J. Research Institute of Chemistry, International Center for Chemical and Biological Sciences, University of Karachi, Karachi-75270, Pakistan, ^bFaculty of Pharmacy, Universiti Kebangsaan Malaysia, Jalan Raja Muda Abdul Aziz, 50300, Kuala Lumpur, Malaysia, ^cDr. Panjwani Center for Molecular Medicine and Drug Research, International Center for Chemical and Biological Sciences, University of Karachi, Karachi-75270, Pakistan, ^dDepartment of Chemistry, Hazara University, Mansehra, Khyber Pakhtunkhwa, Pakistan, ^eHeidelberg Institute for Theoretical Studies, (HITS), GmbH, Schloss-Wolfsbrunnengasse 35, 69118 Heidelberg, Germany, ^fPCSIR Laboratories Complex, Karachi, Shahr-e-Dr. Salimuzzaman Siddiqui, Karachi-75280, Pakistan, ^gAgriculture Research Station, Virginia State University, Petersburg, VA 23806, USA, ^hInterfakultäres Institut für Biochemie, Universität Tübingen, Hoppe-Seyler-Str. 4, 72076 Tübingen, Germany

Abstract

Benzothiazole and its natural or synthetic derivatives have been used as precursors for several pharmacological agents for neuroprotective, anti-bacterial, and anti-allergic activities. The objective of the present study was to evaluate effects of Benzothiazole analogs (compounds **1-26**) for their immunomodulatory activities. Eight compounds (**2, 4, 5, 8-10, 12, and 18**) showed potent inhibitory activity on PHA-activated peripheral blood mononuclear cells (PBMCs) with IC₅₀ ranging from 3.7 to 11.9 μ M compared to that of the standard drug, prednisolone < 1.5 μ M. Some compounds (**2, 4, 8, and 18**) were also found to have potent inhibitory activities on the production of IL-2 on PHA/PMA-stimulated PBMCs with IC₅₀ values ranging between < 4.0 – 12.8 μ M. The binding interaction of these compounds was performed through *in silico* molecular docking. Compounds **2, 8, 9, and 10** significantly suppressed oxidative burst ROS production in phagocytes with IC₅₀ values between < 4.0 and 15.2 μ M. The lipopolysaccharide (LPS)-induced

*Corresponding authors: E-mail: hassaan2@super.net.pk; khalid.khan@iccs.edu; mmesaik@hotmail.com

nitrites in murine macrophages cell line J774 were found to be inhibited by compounds **4**, **8**, **9**, and **18** at a concentration of 25 $\mu\text{g}/\text{mL}$ by 56%, 91%, 58%, and 78%, respectively. Furthermore, compounds **5**, **8**, **12**, and **18** showed significant ($P < 0.05$) suppressive activity on Th-2 cytokine, interleukin 4 (IL-4) with an IC_{50} range of < 4.0 to 40.3 μM . Interestingly compound **4** has shown a selective inhibitory activity on IL-2 and T cell proliferation (naïve T cell proliferation stage) rather than on IL-4 cytokine, while compound **12** displayed an interference with T-cell proliferation and IL-4 generation. Moreover compound **8** and **18** exert non-selective inhibition on both IL-2 and IL-4 cytokines, indicating a better interference with stage leading to humoral immune response and hence possible application in autoimmune diseases.

Keywords: Benzothiazoles, T-cell proliferation, cytokines, molecular docking, ROS and Nitric oxide.

1. Introduction

Benzothiazole derivatives, natural or synthetic, exhibit a variety of biological activities and, therefore, have been used as precursors for pharmacological agents for neuroprotective, anti-bacterial, anti-allergic, immunosuppressive, and antiviral [1-6]. [18,19]. In addition, benzothiazole and its derivatives are powerful antitumor agents. For example, phenylbenzothiazoles, which have been synthesized as pro-drugs, were chosen for clinical evaluation for anti-cancer activity [7-9]. A few other derivatives of benzothiazoles, especially quinol and 2-(4-aminophenyl), have shown anti-cancer activities both, in *in vivo* and *in vitro* systems [10-13]. Recently, a fluorinated 2-arylbenzothiazole was found to have selective and potent inhibitory activity against colon, lung, and breast cancer cells [14]. In contrast, some amino benzothiazoles have been shown to possess mutagenic potency depending on metabolic activation [15] or to induce DNA damage [16]. For example, 2-*p*-tolyl-benzothiazoles and 2-*m*-tolyl-benzothiazoles exhibited mutagenic activity in the T100 strain of *Salmonella* [17]. At cellular levels, benzothiazole inhibit muscarinic receptor activation, lymphocyte-specific protein tyrosine kinase (lck) and calmodulin (CaM) activities [20]. In continuation of our ongoing research on the chemistry and bioactivity of new heterocyclic compounds, we reported recently β -glucuronidase inhibitory activity of benzothiazole analogs [21].

The presented work describes re-synthesis and evaluation of the immunomodulatory potential of a series of benzothiazoles (**1-26**), with special emphasis on their effect on the naïve Th cells and Th-2 cytokine (IL-4). We also studied their effects on phytohemagglutinin (PHA)-induced proliferation of T-cells and on IL-2 production in order to evaluate their therapeutic potential on immune modulation, because the mediators of immune response, when overproduced, can cause serious damage including inflammation and injury [22]. With molecular docking protocols, the binding patterns of IL-2 inhibitors at the IL-2 receptor alpha (IL-2R α) binding site [23,24] is demonstrated. Using the GOLD docking program, the active IL-2 inhibitors were docked at the ligand binding site of IL-2 protein and the mode of interaction was determined [25]. Furthermore, the effect of these compounds on the production of the short-lived nitric oxide radical, [26], and the production of reactive oxygen species, in human peripheral blood phagocytes [27], was determined. Additionally, the effect of these compounds on IL-4 production and their potential cytotoxic effects for normal cell lines were evaluated.

2. Results and Discussion

2.1. Chemistry

Re-synthesis of the benzothiazoles derivatives **1-26** was carried out by reacting 2-aminothiophenol with different aromatic aldehydes in *N, N*-dimethylformamide (DMF) as reported previously [21]. In this reaction, sodium metabisulfite (Na₂S₂O₅) was added to a stirred solution of 2-aminothiophenol (3.12 mmol) and a suitably-substituted aromatic aldehyde (3.16 mmol) in DMF. The resulting reaction solution was refluxed for 2 h. The progress of reaction was monitored by TLC. After completion, the reaction was allowed to cool to room temperature. After addition of water (30 mL), the benzothiazole derivatives **1-26** (Scheme-1) precipitated, and were collected by filtration. Re-crystallization from methanol yielded pure products (Table-1). The structures of compounds **1-26** were confirmed by different spectroscopic methods including ¹H NMR and EI mass spectroscopy and found to match with the data as described previously [21].

Insert Scheme-1 Here

Insert Table-1 Here

2.2. *Effect on T-Cell Proliferation*

Efficacy of benzothiazoles on T-cells was tested using the T-cell proliferation assay. Eight compounds, **2**, **4**, **5**, **8-10**, **12**, and **18**, showed significant suppressive activities ($P < 0.005$) compared to that of the standard drug prednisolone ($IC_{50} = < 1.5 \mu M$) [28] with IC_{50} values of 11.5 ± 1.2 , 10.1 ± 0.4 , 11.9 ± 0.9 , 4.5 ± 0.4 , 4.9 ± 0.1 , 4.1 ± 0.4 , 3.7 ± 0.4 , and $7.5 \pm 1.5 \mu M$, respectively (Figure-1). The inhibitory activity on T-cell immune response of these compounds might be useful as lead molecules for the development of drugs against various immune disorders.

Insert Figure-1 Here

2.3. *Effect on Th cells (Naïve) IL-2 cytokine*

Compounds that showed inhibitory activity on the proliferation of T-cells were also tested for their effect on the production of IL-2 by T-cells because IL-2 acts as a growth factor for T-cells. Compounds **2**, **4**, **5**, **8**, and **18** were found to suppress IL-2 production significantly ($p < 0.005$, < 0.05), when compared to that of the mock control (activated cells without addition of compounds). Four compounds, **2**, **4**, **8**, and **18**, were found to have potent inhibitory activity with IC_{50} values of < 4.0 , 12.8 ± 3.1 , < 4.0 , and $4.2 \pm 0.4 \mu M$, respectively. Compound **5** had a slightly lower level of inhibition as compared to the afore-mentioned compounds with IC_{50} of $26 \pm 3.5 \mu M$ (Figure-2).

Insert Figure-2 Here

2.4. *Effect on ROS generation*

Compounds **1-26** were screened for immunomodulatory ROS activity. Out of twenty-six screened compounds, only four (**2**, **8-10**) showed significant inhibitory activity on ROS generation with IC_{50} values of 7.4 ± 2.3 , < 4.0 , 15.2 ± 0.8 , and $4.5 \pm 0.4 \mu M$, respectively. These values were superior to the standard Ibuprofen ($IC_{50} = 57.2 \pm 5.8 \mu M$). The compounds **13**, **14**, **20**, and **24** showed moderate inhibitory activity on ROS generation with IC_{50} values of $45.6 \pm$

3.7, 46.4 ± 4.7 , 73 ± 0.5 , and $66.3 \pm 11.5 \mu\text{M}$, respectively (Table-2). The remaining compounds were found to be inactive, exhibiting less than 50% of inhibition. These results demonstrate that the compounds could potentially exert an inhibitory effect on the innate immune response.

2.5. Effect on NO production

The effect of these compounds on nitric oxide accumulation by stimulated macrophages was also determined. Lipopolysaccharide (LPS)-treated J774.2 mice macrophages are widely used to study the mechanisms of nitric oxide synthase (NOS-2) induction. Data shown in Table 2 and Figure 3 indicates that out of twenty-six compounds tested, four of them, compounds **4**, **8**, **9**, and **18** showed very potent inhibition at 25 mM concentration on NO production with percentages of inhibition of 56.1 ± 0.6 , 91.1 ± 0.7 , 58.5 ± 3.3 , and 78.1 ± 1.6 , respectively (Table-2 and Figure-3). Furthermore, the IC_{50} values for compounds **4**, **8**, **9**, and **18** were found to be 34.8 ± 4.0 , < 20 , 51.8 ± 8.6 , and $126 \pm 16.6 \mu\text{M}$, respectively. If NO is overproduced it reacts with superoxide and gives rise to the very toxic radical peroxynitrite which may play a role in many diseases with an autoimmune etiology. So, the suppression of NO could be a suitable target toward inflammatory diseases.

Insert Table-2 Here

2.6. Effect on IL-4 cytokine

In order to study the target specificity of the compounds that inhibit the T-cell proliferation, the Th-2 cytokine (IL-4) production was determined which act as a growth supporting factor for B cells proliferation beside IL-2. Only compound **12** showed potent inhibitory activity with an IC_{50} value of $< 4.0 \mu\text{M}$, whereas compound **5**, **8**, and **18** had moderate inhibitory activities with IC_{50} values of 39.2 ± 2.6 , 40.3 ± 2.5 , and $31 \pm 0.4 \mu\text{M}$, respectively (Figure-4). Although compounds **2**, **4**, **5**, **8**, and **18** suppress production of IL-2, not a similar inhibitory activity for the IL-4 production was observed. This effect reflects that these compounds specifically inhibit the *Th* cells (*Naïve*) IL-2 cytokine rather than Th-2 cytokines (IL-4 in particular).

Insert Figure-4 Here

2.7. Cytotoxicity

To determine the cytotoxic effect of those compounds on normal cells, the MTT assay was performed using the normal mouse fibroblast cell line 3T3 NIH. We observed that except **18** all of the tested compounds **2**, **4**, **5**, **8**, **10**, **14**, and **24** did not suppress the growth of 3T3 cells even at the highest concentration (100 μM). However, mild cytotoxicity was shown with compounds **9** and **13**. Compound **18** showed a cytotoxic activity with an IC_{50} value of $40.1 \pm 5.0 \mu\text{M}$. Therefore, we assume that benzothiazole derivatives can act as anti-inflammatory lead molecules.

2.8. Molecular Docking Studies of IL-2 Inhibitors

Molecular docking is the most widely used computational tool to identify protein-ligand interactions [29] and gain insights into the molecular mechanism of protein-ligand binding, e.g. to determine the binding orientation of active IL-2 inhibitors into the ligand binding site. The cytokine IL-2 binding site is a heterotrimeric receptor complex consisting of α , β and γ chains (IL-2R α , IL-2R β and IL-2R γ). Reported studies suggest that antibodies that block IL-2-IL-2R α binding have effective clinical implication [30, 31]. Therefore, the new IL-2 inhibitors were targeted against the IL-2R α binding site which is dissected into two distinct sub-sites; the first is relatively fixed and includes the center of helix B and the A'-B loop and the other is highly mobile which comprises the C-terminus of helix B, the loop connecting helices A and A', and the loop connecting helix B to helix C [35]. Prior to the docking of compounds **2**, **4**, **5**, **8**, and **18**, the co-crystallized compound (phenylalanine methyl ester derivative) was successfully re-docked into the ligand binding site of the protein with a RMSD value of 1.2 Å. The results are displayed in supporting information. The re-docking analysis suggested that the Swiss Dock docking server was able to predict the known binding conformation accurately and can be used to elucidate the binding patterns of our synthesized compounds. The docked binding modes of compounds **2**, **4**, **5**, **8**, and **18** revealed that all these compounds fit into the cavity formed between the A and A' helix and B helix (Fig 5a). The binding site residues lying within 5 Å for all five active compounds were found to be Lys32, Pro31, Arg35, Meth36 (A' helix) and the hydrophobic residues Val66 and Leu69 (residing on B helix). The dock poses of the active compounds reflected that Arg35 and Lys32 are important for hydrogen bonding with the benzothiazole ring and the substituted phenyl ring containing a hydroxyl or methoxy group. Moreover, two important amino acid residues from the B helix (Val66 and Leu69) showed hydrophobic

interactions with the aromatic ring of the benzothiazol skeleton (Fig 5b). Additional π - π interactions exist between the aromatic rings of the ligands Phe39 C-terminus of the A' helix. These interactions were expected to be clearly observed during molecular dynamics simulation due to possible side chain flipping and reorientation of the ligand in the binding pocket. These adaptable changes may help in stabilization of these compounds by providing π - π interactions. The docked binding modes of five active compounds and side chain residues interacting with ligand 2 are shown in Figures 5a-c.

Insert Figure-5a Here

Insert Figure-5b Here

Insert Figure-5c Here

2.9. *Molecular Dynamics Simulation:*

To further validate and confirm the binding mode of ligands predicted by Swiss Dock, molecular dynamics (MD) simulation studies were carried out in aqueous medium. A total of 15 ns MD simulations were performed in an explicit solvent model. Results were analyzed to check the overall structural stability by using root mean square deviation (RMSD) and the energy output. The structure seems to be stable after 2 ns of unrestrained equilibration. RMSD for all backbone atoms was calculated by using a minimized structure as a reference point and it showed RMSD convergence around 1.75 Å with slight fluctuations, which were expected due to highly mobile loop regions discussed earlier. Fluctuation for each residue was carried out using the B-factor analysis which showed major flexibility for the residues forming loop regions, whereas ligand binding region seemed to be stable. The energy output was calculated using perl script which showed an increase in the potential energy during heating, but after that it was decreased during equilibration and remained stable during production run. Trajectories were visualized by using VMD software (Figure-6).

Insert Figure-6 Here

The binding mode of ligands was analyzed for entire trajectories which showed no difference from initial conformation and remained stable in the binding pocket as identified by Swiss Dock. The superposition of starting structure with last snapshot of 15 ns simulation was performed to see any dynamic change adopted by the ligand during simulation. Although the ligand tries to

adopt different conformations, it returns back to the original position. This may be due to its strong hydrophobic interaction between V66 and L69 residues with the benzothiazole skeleton. At the some point aromatic interactions are visible between F39, which flips closer to the benzene ring of the ligand (Figure-6). From MD simulation studies, we observed stable interactions between ligand and its binding pocket residues which was maintained throughout the simulation. A further detailed MD simulation study is beyond the scope of this manuscript.

Insert Table-3 Here

3. Conclusion:

All twenty six benzothiazoles were tested on various assays and it was found that some derivatives show potent inhibitory potential for the generation of IL-2, IL-4, ROS, and NOS. Eight compounds, **2, 4, 5, 8-10, 12, and 18**, exhibited dose-dependent suppressive activities on PHA-activated T-cell proliferation.. However, only compounds **2, 4, 5, 8, and 18** were found to suppress IL-2 .production, whereas compound **12** showed potent inhibitory activity on IL-4 generation beside T cell proliferation inhibition. Compounds **2, 8-10** showed a potent inhibitory activity on ROS formation compared to that of the standard control (ibuprofen). Compounds **4, 8, 9, and 18** were also acted as highly potent inhibitors for NO generation as well. IL-2 functions as a master regulator to direct for cell fate through priming for differentiation and maintaining the differentiated state. One of tragic effects of IL-2 is promotion of inflammatory responses which is mainly maintained through the generation of Th1 and Th2 effector cells. These effects could be reduced through selective inhibition. From these results we can observe compounds **4 and 12** to exert selective inhibition on IL-2, IL-4, respectively. Additionally compound **8 and 18** exert non-selective inhibition on IL-2 as well as on IL-4 cytokines indicating a better interference with stage leading to humoral immune response. While compound **4** found effecting merely the naïve T cell proliferation stage. Consequently, *in silico* studies were performed to recognize the binding mode of these compounds. The planned scaffold of immunomodulatory agents deals with the possibility of further beneficial modifications that could give rise to lead molecules with improved inhibitory activity and selectivity. Cytotoxicity of the above identified

immunosuppressive compounds was excluded by MTT, as assayed by the murine fibroblast cell line 3T3 of NIH. Therefore, we anticipate that the benzothiazole derivatives which were evaluated in the present study, can act as valuable anti-inflammatory/immunosuppressive lead agents. However, the exact mode of action of these compounds and the detail of activities deserve detail investigations which are in progress.

4. Experimental Section

4.1. *Materials and Methods*

All reagents and solvents were purchased from E. Merck, Germany and were of analytical grade. NMR experiments were performed on an Avance Bruker AM 300 MHz machine. CHN analyses were carried out on a Carlo Erba Strumentazione-Mod-1106, Milano, Italy. Ultraviolet (UV) spectra were recorded on a Perkin-Elmer Lambda-5 UV/VIS spectrophotometer in MeOH and infrared (IR) spectra was recorded on a JASCO IR-A-302 spectrometer as KBr discs. Electron impact mass spectra (EI MS) were obtained on a Finnigan MAT-311A (Germany) mass spectrometer. Thin-layer chromatography (TLC) was performed on pre-coated silica gel aluminum plates (Kieselgel 60, 254, E. Merck, Germany). Chromatograms were visualized either by UV at 254 and 365 nm or iodine vapors.

4.2. *General procedure for the synthesis of compounds 1-26*

In a typical reaction, benzothiazoles **1-26** were re-synthesized by dissolving 2-aminothiophenol (3.12 mmol) and different aromatic aldehydes (3.16 mmol) in DMF (10 mL). Sodium metabisulfite ($\text{Na}_2\text{S}_2\text{O}_5$, 0.61 g) was also added to the above-mentioned solution with continuous stirring. The resulting reaction mixture was refluxed for 2 h and the progress of the reaction was monitored by TLC analysis. After completion of the reaction, it was allowed to cool to room temperature and water (30 mL) was added. The solid precipitated benzothiazoles (**1-26**) were collected on a filter and obtained in high yields. Recrystallization from methanol yielded pure products and their physical and spectroscopic data matched satisfactorily with previously reported literature values [21].

4.3. *T-cell proliferation assay*

Fresh venous blood from healthy donors was mixed with an equal volume of incomplete RPMI-1640 media (Mediatech Inc., Herndon, VA, USA) containing 2 mM L-glutamine and 1%

penicillin/streptomycin. The diluted blood was then layered onto lymphocyte separation medium (MP Biomedicals, Inc., Ohio, USA) and centrifuged at 400 g for 20 min at 25 °C. The mononuclear cell layer was collected, washed with RPMI-1640 and centrifuged at 300 g for 10 min at 4 °C. The peripheral mononuclear blood cells (PBMNCs) were re-suspended in RPMI-1640 complete medium containing 10% fetal bovine serum (PAA laboratories GmbH, Pasching, Austria). In a 96-well round-bottomed plate (Iwaki, Scitech. DIV., Ashai Techno Glass, Japan), 50 μ L of cell suspension (2.5×10^6 cell/mL), 50 μ L of phytohemagglutinin (PHA) for a final concentration of 5 mM, 50 μ L of supplemented RPMI-1640 along with 50 μ L of test compounds in a final concentration of 0.5, 5 and 50 mM (in triplicates) were added to the culture mixture. Plates were then incubated at 37 °C in a humidified atmosphere of 5% CO₂ in air for 72 h. To each well, 0.5 μ Ci [methyl-³H]-thymidine (Amersham Place Little Chalfont, Buckinghamshire, UK) was added for an additional 18 h. Cells were harvested using a cell harvester (Inotech, Dottikon, Switzerland), and the level of radioactive [methyl-³H]-thymidine incorporated in newly synthesized DNA was measured using a liquid scintillation counter (Beckman coulter, LS 6500, Fullerton, CA, USA).

4.4. Interleukin-2 (IL-2) assay

The PBMCs were cultured in a 96-well flat-bottomed plate (1.0×10^5 cell/well) in the presence or absence of three concentrations of test compounds (1.0, 5.0, and 20 mM) with phytohemagglutinin (PHA) and phorbol myristate acetate (PMA) in a final concentration of 5 mM and 20 mM, respectively. After an incubation period of 18 h at 37 °C in a humidified atmosphere of 5% CO₂ in air, the supernatant was collected for IL-2 determination. Interleukin-2 levels were measured using an enzyme-linked immunosorbent assay (ELISA; R&D Systems, Minneapolis, MN, USA). The assay was performed according to the manufacturer's instructions. Briefly, a 96-well flat-bottomed ELISA plate was coated with 4.0 mM mouse anti-human IL-2 in PBS, pH 7.4. Then, re-combinant human IL-2 standards and culture supernatant samples were added and incubated for 2 h followed by washing steps and finally addition of biotinylated goat anti-human IL-2. After an incubation period of 2 h at room temperature, the plates were again washed and streptavidin-conjugated horseradish peroxidase was added to each well and the plates were incubated for additional 20 min at room temperature. After final washing, an enzyme substrate solution of H₂O₂ and tetramethylbenzidine (1:1 v/v) was added, and the color was allowed to develop at room temperature in the dark. The plates were then read at 450 nm in a

plate reader (DIAREader GMBH, Wiener, Neudorf, Austria). The results were analyzed using the Microsoft Excel Program.

ACCEPTED MANUSCRIPT

4.5. Chemiluminescence assay (ROS)

Formation of reactive oxygen species (ROS) in whole blood during the oxidative burst was determined by the luminol-enhanced chemiluminescence assay [32]. In brief, three concentrations of each compound (1.0, 10, and 100 mM) were prepared in 25 μL of Hank's balanced salt solution containing calcium chloride and magnesium sulfate (HBSS⁺⁺) in a half area 96-well white flat-bottomed plate (Sigma Aldrich, Steinheim, Germany) for a final volume of 100 μL . Then 25 μL of whole blood diluted 1:50 in a suspension of HBSS⁺⁺ was added. Positive (zymosan-activated cells), negative controls (non-activated cells) and blank wells were included. Cells and compounds were incubated for 30 min at 37 °C, then 25 μL luminol (3-aminophthalhydrazide; Research Organics Cleveland, Ohio, USA), was added into each well followed by addition of 25 μL of serum-opsonized zymosan (*Saccharomyces cerevisiae* origin; Fluka, Buchs, Switzerland) except for negative and blank wells. The ROS chemiluminescence kinetic was monitored with a luminometer from Labsystems (Helsinki, Finland), for 50 minutes in the repeated scan mode. Peak and total integral chemiluminescence readings were expressed in the relative light unit.

4.6. Nitrite concentration in Mouse Macrophage Culture Medium

The mouse macrophage cell line J774.2, obtained from ECACC, Salisbury, Wiltshire (UK), was cultured in T75 flasks in Dulbecco's Modified Eagle Medium (DMEM) containing 10% fetal bovine serum, supplemented with 1% streptomycin/penicillin. Flasks were kept at 37 °C in the atmosphere of humidified air containing 5% CO₂. Cells were then seeded in a 24-well plate (10⁶ cells/mL), and nitric oxide synthase (NOS2) in the macrophages was induced by the addition of 20 mM *E. coli* lipopolysaccharide (LPS) (DIFCO Laboratories, Michigan, USA). The test compounds were added at a concentration of 25 mM soon after LPS stimulation and incubated at 37 °C in 5% CO₂. The cell culture supernatant was collected after 24 h. Nitrite accumulation in the J774.2 cell culture supernatants was determined using the Griess method [33], where 50 μL of 1% sulphanilamide in 2.5% phosphoric acid, followed by 50 μL of 0.1% (1-naphtyl) ethylenediamine in 2.5% phosphoric acid were added to 50 μL culture medium. After 10 minutes of incubation at room temperature, the absorbance at 550 nm was read. Micromolar concentrations of nitrite were calculated from a standard curve constructed with sodium nitrite as reference compound. The results are expressed as means \pm SD of three experiments.

4.7. Interleukin-4 (IL-4) assay

The PBMCs were cultured in a 96-well flat-bottomed plate (2.0×10^6 cell/mL) in the presence or absence of three concentrations of test compounds (1.0, 5.0, and 25 mM) and phytohemagglutinin (PHA) in a final concentration of 7.5 mM. After an incubation period of 18 h at 37 °C in 5% CO₂, the supernatant was collected for IL-4 determination. Interleukin-4 levels were determined by using an enzyme-linked immunosorbent assay (ELISA) kit (Diacclone, France). The assay was performed according to the manufacturer's instructions. Briefly, in a 96-well ELISA, coated with monoclonal mouse anti-human IL-4, 100 μ l recombinant human IL-4 standards and culture supernatant samples were added. The plates were incubated for 2 h at room temperature and washed three times with washing buffer, followed by the addition of biotinylated goat anti-human IL-4 and further incubated for 1 h at room temperature. Then, the plates were again washed, and streptavidin-conjugated horseradish peroxidase was added and incubated for an additional 20 min at room temperature. After three final washings, the enzyme substrate solution was added and incubated for 12 to 15 min to allow color development at room temperature in the dark. Then stop solution was added and the plates were read at 450 nm in a plate reader (DIAREader GMBH, Wiener, Neudorf, Austria). The results were analyzed using Microsoft Excel Program.

4.8. Cytotoxicity assessment using MTT assay

In vitro cytotoxicity assays were performed as described previously [34] using the 3T3 NIH mouse embryo fibroblast cell line (American Type Culture Collection 'ATCC, Manassas, VA 20108, USA). The 3T3-NIH cells were suspended in Dulbecco's Modified Eagle's Medium (DMEM) formulated with 10% FBS. In flat-bottomed plates, the cells were plated at a concentration of 6×10^4 cells/mL and incubated for 24 h at 37 °C and 5% CO₂ environment. After removal of media, the cells were challenged with three different concentrations (0.5, 5.0, and 25 mM) of compounds in triplicates and then further incubated for 48 h at 37 °C in a CO₂ incubator. Cell viability was assessed by exposure of 0.5 mM of MTT (3-(4,5-dimethylthiazol-2-yl)-2,5-diphenyltetrazolium bromide) for 4 h followed by the removal of the supernatant and addition of DMSO to solubilize the formazan complex. The plates were read at 540 nm after one minute shaking and readings were processed using MS Excel software Program. The results were expressed as means \pm SD of three experiments.

4.9. Molecular Docking

For investigation of binding modes of IL-2 inhibitors and their interactions at molecular level, docking and all atomic molecular dynamics (MD) simulations were performed. For docking calculations, the crystal structure of interleukin-2 in complex with phenylalanine methyl ester (PDB entry code 1M48) was retrieved from the RCSB Brookhaven Protein Data Bank [35,36]. In the crystal structure of 1M48, residues forming the BC loop (75-80) were missing which were modeled by transferring coordinates from IL-2 PDB structure (3INK) using PYMOL software. The modeled structure was run for short minimization using the AMBER12 software package which was then used as starting structure for docking studies. All water molecules were removed from the original PDB crystal structure and hydrogen atoms were added by default program in tleap during minimization. Ligand structures were constructed by using the ChemDraw program and converted into 3D using babel 2.2. Geometry optimizations for the 3D structures were performed using Tripos force field with a distance-dependent dielectric and the Powell conjugate gradient algorithm [37]. Gasteiger-Hückel charges were used for the ligands. Online web server Swiss Dock was used for docking studies of experimentally-determined active compounds (**2**, **4**, **5**, **8**, and **18**) which a separate pdb file for protein and mol2 files for ligands were uploaded and default parameters were selected to perform docking on the whole protein. After the docking assay was completed a zip file was generated for showing various binding modes. UCSF Chimera was used for visualization of binding modes.

4.10. Molecular Dynamics Simulations

On basis of highest ranking binding mode (BMs) of ligands with IL-2, generated by Swiss Dock, we selected ligand **2** for further confirmation of active site residue interactions using explicit solvent molecular dynamics simulations. The docked complex was prepared in tleap package in AMBER 12 (Amber generalized force field for organic molecules) using FF99SB and GAFF for protein-ligand complex, respectively. Before using tleap all the parameters for ligand were prepared in antechamber program given in AMBER package. The system was solvated by using a TIP3P octahedral 10 Å water box which added a total of 7014 water residues, making up a total system of 23220 atoms. Energy minimization was performed in two stages: firstly by applying a positional restrain weight of 500 kcal/mol·Å² on all atoms except for hydrogen (1000 steps of steepest descent minimization and 4000 steps of conjugate gradient methods), second by step

minimization (10,000 steps), done by simply releasing restraint weight from all atoms. The heating was performed by slowly increasing temperature from 10 to 300 K using NVT ensemble in 25 ps with position restraint applied on all heavy atoms ($50 \text{ kcal/mol}\cdot\text{\AA}^2$). During heating integration the time step was set to 1 fs and Langevin dynamics collision frequency $\gamma = 1$. Heating was followed by 200 ps equilibration under NPT ensemble with slowly decreasing the force of restraint on heavy atoms from $50 \text{ kcal/mol}\cdot\text{\AA}^2$ to 0 in 8 steps. During equilibration, temperature and pressure were kept constant at 300 K and 1.0 bar by applying Langevin thermostat and isotropic position rescaling, respectively, at 1ps relaxation time. Finally, all the restraints were removed during 2 ns equilibration with SHAKE algorithm to constrain all the bonds involving hydrogen atoms and integration time was increased to 2 fs. The MD simulation was performed by keeping particle mesh ewald (PME) on, and non-bonded interactions were truncated at a cut off value of 10 Å.

Acknowledgement:

The authors are thankful to the Higher Education Commission (HEC) Pakistan (Projects No. 20-2073) for financial support and to DAAD (Deutscher Akademischer Austauschdienst), Bonn, (Germany) for fellowship grant to Prof. Dr. Khalid M. Khan.

References:

1. Y.J. Cao, J.C. Dreixler, J.J. Couey, and K.M. Houamed, Modulation of recombinant and native neuronal SK channels by the neuroprotective drug riluzole. *Euro. J. Pharmacol.* 449 (2002) 47-54.
2. A.D. Ramirez, S.K.F. Wong, F.S. Menniti, Pramipexole inhibits MPTP toxicity in mice by dopamine D3 receptor dependent and independent mechanisms. *Bioorg Med Chem.* 475 (2003) 29-35.
3. M.H. Jung, S.W. Choi, J.G. Park, K.W. Cho, J.Y. Kong, Studies of muscarinic receptor agonists: 2-(1-methyl-1,2,3,6-tetrahydropyridin-4-yl) benzoxazoles/benzothiazole *Korean. J. Med. Chem.* 9 (1999) 56-62.

4. J. Das, R.V. Moquin, J. Lin, C. Liu, A.M. Doweiko, H.F. DeFex, Q. Fang, S. Pang, S. Pitt, D.R. Shen, Discovery of 2-amino-heteroaryl-benzothiazole-6-anilides as potent p56lck inhibitors. *Bioorg. Med. Chem. Let.* 13 (2003) 2587-2590.
5. G. Turan-Zitouni, Synthesis of some 2-[(benzazole-2-yl) thioacetyl-amino] thiazole derivatives and their antimicrobial activity and toxicity. *Eur. J. Med. Chem.* 39 (2004) 267-272.
6. M. Ban, H. Taguchi, T. Katsushima, M. Takahashi, K. Shinoda, A. Watanabe, T. Tominaga, Novel antiallergic and anti-inflammatory agents. Part I: Synthesis and pharmacology of glycolic amide derivatives. *Bioorg. Med. Chem.* 6 (1998) 1069-1076.
7. I.H. Hall, N.J. Peaty, J.R. Henry, J. Easmon, G. Heinisch, G. Pürstinger, Investigations on the mechanism of action of the novel antitumor agents 2-benzothiazolyl, 2-benzoxazolyl, and 2-benzimidazolyl hydrazones derived from 2-acetylpyridine. *Arch. Pharm. (Weinheim)*. 332 (1999) 115-123.
8. T.D. Bradshaw, A.D. Westwell, The development of the antitumour benzothiazole prodrugs, Phortress, as a clinical candidate. *Curr. Med. Chem.* 11 (2004) 1009-1021.
9. A.D. Westwell, The therapeutic potential of aryl hydrocarbon receptor (AhR) agonists in anticancer drug development. *Drugs of the Future*. 29 (2004) 479-491.
10. G. Wells, T.D. Bradshaw, P. Diana, A. Seaton, D.F. Shi, A.D. Westwell, M. F.G. Stevens, Antitumour benzothiazoles. Part 10: the synthesis and antitumour activity of benzothiazole substituted quinol derivatives. *Bioorg. Med. Chem. Let.* 10 (2000) 513-515.
11. C.D. Hose, M. Hollingshead, E.A. Sausville, A. Monks, Induction of CYP1A1 in tumor cells by the antitumor agent 2-[4-amino-3-methylphenyl]-5-fluoro-benzothiazole: a potential surrogate marker for patient sensitivity. *Molecul. Cancer Therap.* 2 (2003) 1265-1272.
12. C.O. Leong, M. Gaskell, E.A. Martin, R.T. Heydon, P.B. Farmer, M.C. Bibby, P.A. Cooper, J.A. Double, T.D. Bradshaw, M.F.G. Stevens, Antitumour 2-(4-aminophenyl) benzothiazoles generate DNA adducts in sensitive tumour cells in vitro and in vivo. *British J. Cancer* 88 (2003) 470-477.

13. E. Brantley, V. Patel, S. F. Stinson, V. Trapani, C.D. Hose, H.P. Ciolino, G.C. Yeh, J.S. Gutkind, E.A. Sausville, A.I. Loaiza-Pérez, The antitumor drug candidate 2-(4-amino-3-methylphenyl)-5-fluorobenzothiazole induces NF-[kappa] B activity in drug-sensitive MCF-7 cells. *Anti-Cancer Drugs* 16 (2005) 137-142.
14. C.G. Mortimer, G. Wells, J.P. Crochard, E.L. Stone, T.D. Bradshaw, M.F. G. Stevens, A.D. Westwell, Antitumor benzothiazoles. 26. 2-(3, 4-Dimethoxyphenyl)-5-fluorobenzothiazole (GW 610, NSC 721648), a simple fluorinated 2-arylbenzothiazole, shows potent and selective inhibitory activity against lung, colon, and breast cancer cell lines. *J. Med. Chem.* 49 (2006) 179-185.
15. G. Sato, S. Asakura, A. Hakura, Y. Tsutsui-Hiyoshi, N. Kobayashi, K. Tsukidate, Assessment of potential mutagenic activities of a novel benzothiazole MAO-A inhibitor E2011 using *Salmonella typhimurium* YG1029. *Mutat. Res.* 472 (2000) 163-169.
16. B. Ayaz Tuylu, H.S. Zeytinoglu, I. Isikdag, Synthesis and mutagenicity of 2-aryl-substitute (*o*-hydroxy-, *m*-bromo-, *o*-methoxy-, *o*-nitro-phenyl or 4-pyridyl) benzothiazole derivatives on *Salmonella typhimurium* and human lymphocytes exposed in vitro. *Clinic. Cancer Res.* 62 (2007) 626-632.
17. H. Zeytinoglu, A. Meric, B. Tuylu, E. Ergene, Synthesis and genotoxic activities of five 2-aryl-substitutedbenzothiazole derivatives. *Rev. Chim.* 57 (2006) 1247-1252.
18. A.R. Carroll, P.J. Scheuer, Kuanoniamines A, B, C, and D: Pentacyclic alkaloids from a tunicate and its prosobranch mollusk predator *Chelynotus semperi*. *J. Org. Chem.* 559 (1990) 4426-4431.
19. G.P. Gunawardana, S. Kohmoto, S.P. Gunasekera, O.J. McConnell, F.E. Koehn, Dercitine, a new biologically active acridine alkaloid from a deep water marine sponge, *Dercitus* sp. *J. Am. Chem. Soc.* 110 (1988) 4856-4858.
20. T. Tanaka, H. Umekawa, M. Saitoh, T. Ishikawa, T. Shin, M. Ito, H. Itoh, Y. Kawamatsu, H. Sugihara, H. Hidaka, Modulation of calmodulin function and of Ca²⁺-induced smooth muscle contraction by the calmodulin antagonist, HT-74. *Molecul. Pharmacol.* 29 (1986) 264-269.

21. K.M. Khan, F. Rahim, S.A. Halim, M. Taha, M. Khan, S. Perveen, H. Zaheer, M. A. Mesaik, M. I. Choudhary, *Bioorg. Med. Chem.* 19 (2011) 4286-4294.
22. B. Sadlack, H. Merz, H. Schorle, A. Schimpl, A.C. Feller, and I. Horak, *Cell*, 75 (1993) 253-261.
23. E.S.H. El Ashry, M.R. Amer, O.M. Abdalla, A.A. Aly, S. Soomro, A. Jabeen, S.A. Halim, M.A. Mesaik, H. Zaheer, *Bioorg. Med. Chem. Bioorg Med Chem.* 20 (2012) 3000-3008.
24. M.A. Mesaik, A. Jabeen, S.A. Halim, A. Begum, A.S. Khalid, M. Asif, B. Fatima, H. Zaheer, M. I. Choudhary, *Chem. Biol. Drug Des.* 79 (2012) 290–299.
25. GOLDv3.0. Cambridge Crystallographic Data Center, Cambridge, UK. (2006).
26. C. Nathan, Nitric oxide as a secretory product of mammalian. *FASEB J.* 6 (1992) 3051-3064.
27. E.J. Swindle, J.A. Hunt, Coleman. Comparison of Reactive Oxygen Species Generation by Rat Peritoneal Rat Peritoneal Macrophages and Mast Cells Using the Highly Sensitive Real-Time Chemiluminescent Probe Pholasin: Inhibition of Antigen-Induced Mast Cell Degranulation by Macrophage-Derived Hydrogen Peroxide. *J. Immunol.* 169 (2002) 5866-5873.
28. El Ashry el SH1, El Tamany el SH, Abd El Fattah Mel D, Aly MR, Boraie AT, Mesaik MA, Abdalla OM, Fatima B, Jabeen A, Shukrulla A, Soomro S. *J Enzyme Inhib Med Chem.*;28 (2013):105-112.
29. S. Y. Huang, X. Zou, *Protein Sci.* 16 (2007) 43-51.
30. T. A. Waldmann, *Immunol. Today* 14 (1993) 264-270.
31. J. Hakimi, D. Mould, T. A. Waldman, C. Queen, C. Anasetti, S. Light, In *Antibody Therapeutics*; W. J. Harris, J. R. Eds. Adair, CRC Press: Boca Raton, FL. (1997) 277-300.
32. S.L. Helfand, J. Werkmeister, J.C. Roder, *J. Exp. Med.* 156 (1982) 492-505.
33. M.A. Andrade, M.S. Lucas, J.L.P. Arellano, C.P. Barreto, B. Valladares, E. Espinoza, A. Muro, *Nitric Oxide* 13 (2005) 217-225.

34. D.A. Scudiero, R.H. Shoemaker, K.D. Paull, A. Monks, S. Tierney, T.H. Nofziger, M.J. Currens, D. Seniff, M.R. Boyd, *Cancer Res. Sep. 148 (1988) 4827-4833.*
35. H.M. Berman, J. Westbrook, Z. Feng, G. Gilliland, T.N. Bhat, H. Weissig, I.N. Shindyalov, P.E. Bourne, *Nucl. Acids. Res. 28 (2000) 235-242.*
36. R. Michelle, M. Arkin, W. L. Randal, J. DeLano, T. N. Hyde, J. D. Luong, D. R. Oslob, L. Raphael, J. W. Taylor, S. M. Robert, A. W. James and C. B. Andrew, *Proc. Natl. Acad. Sci. U S A. 100 (2003) 1603-1608*
37. SYBYL Molecular Modeling Software version 7.3, Tripos Associates, St. Louis. MO. (2006).

ACCEPTED MANUSCRIPT

Captions:**Scheme-1:** Synthesis of Benzothiazole derivatives 1-26

Figure-1: Effect of compounds **2, 4, 5, 8-10, 12, and 18** on T-cell proliferation. PBMNCs were stimulated with 5 μ g PHA in the presence of three concentrations of test compounds or without addition of compounds (+ve). Cell proliferation was assessed as indicated in the section Materials and Methods. The figure represents compounds that show potent activity against T-cell proliferation the bars indicate mean radioactivity (CPM) \pm SD of triplicate measurements. Significance difference was calculated in comparison with the PHA positive control (+ ve), $P < 0.005^{**}$, $P < 0.05^{*}$. -ve: control cells without PHA or compound.

Figure-2: Concentration-response graph for IL-2 production by PBMNCs. The bars represent the effect of compounds **2, 4, 5, 8, and 18** on IL-2 production by PHA/PMA-stimulated PBMNCs after an incubation of 18 h. Data are mean values \pm S.D (n=3) of produced IL-2 in pg/mL. $P < 0.05^{*}$, $P < 0.005^{**}$

Figure-3: Concentration-response curve for benzothiazoles **4, 8, 9, and 18** on NO production by macrophages-stimulated with LPS in the presence of increasing concentrations of the compounds. Results shown are the mean \pm SD of triplicate measurements expressed as percentage of stimulated control in the absence of compounds.

Figure-4: Effect of benzothiazoles on the production of IL-4 using human peripheral blood mononuclear cells (PMBCs). The graph represents the effect of seven benzothiazoles on PHA-stimulated IL-4 production after 18 h incubation. Each bar represents a mean of triplicate readings. + C: cells in the presence of PHA, - C: cells without PHA.

Figure-5a: Binding orientation of ligand-2, docked in the binding cavity between A' and B helices. Top 9 clusters generated by SwissDock are shown in this figure where the **benzothiazole** skeleton is found to be rigid and shows the same orientation, but only a slight difference in the orientation of the R group, connected to the skeleton by a rotatable bond, is observed.

Figure-5b: Binding of five different ligands superimpose completely on each other. The benzothiazol skeleton shows binding at the same position, while, the R group has a slightly different orientation as seen in the previous figure.

Figure 5c: Superimposed structures of 1M48 with the crystallized ligand FRG (in pink) and docked compound **2** (yellow). The binding site residues interacting with compound **2** (in yellow) within 5 Å distance are shown in magnified area. Main residues from A' (K32, P31, R35, and M36) and B helices (V66 and L69) show interactions with the ligand. All figures were prepared using UCSF Chimera and Pymol software.

Figure-6: RMSD graph shows structural convergence after 1ns equilibration using a minimized structure as a reference point.

Scheme-1:

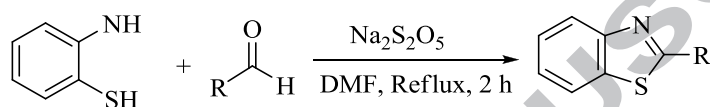


Figure-1:

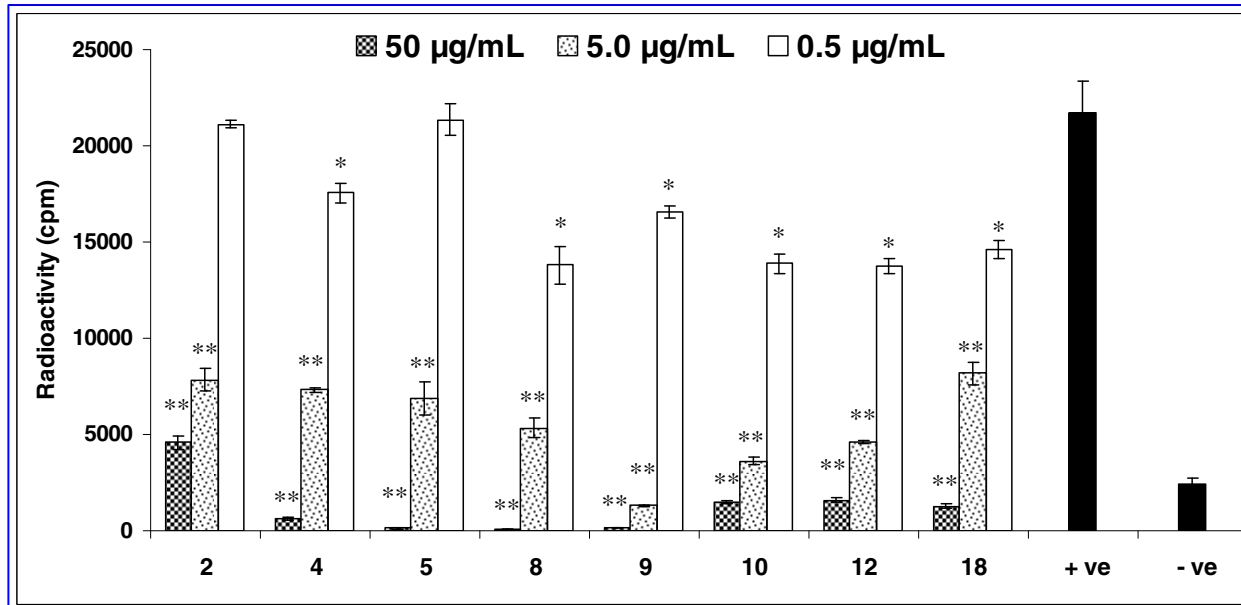


Figure-2:

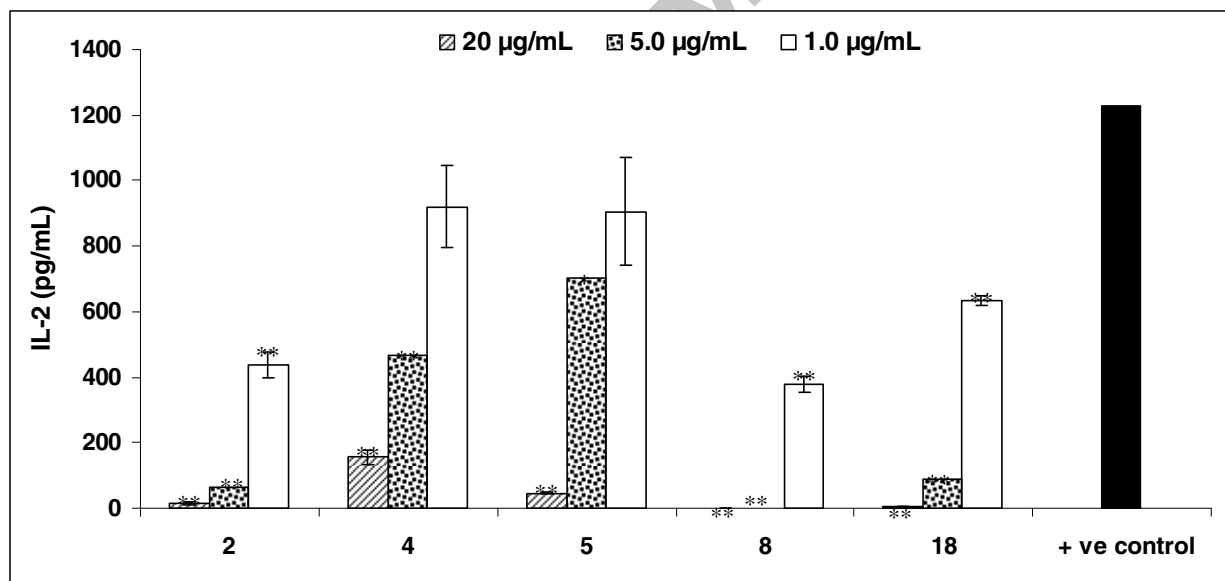


Figure-3:

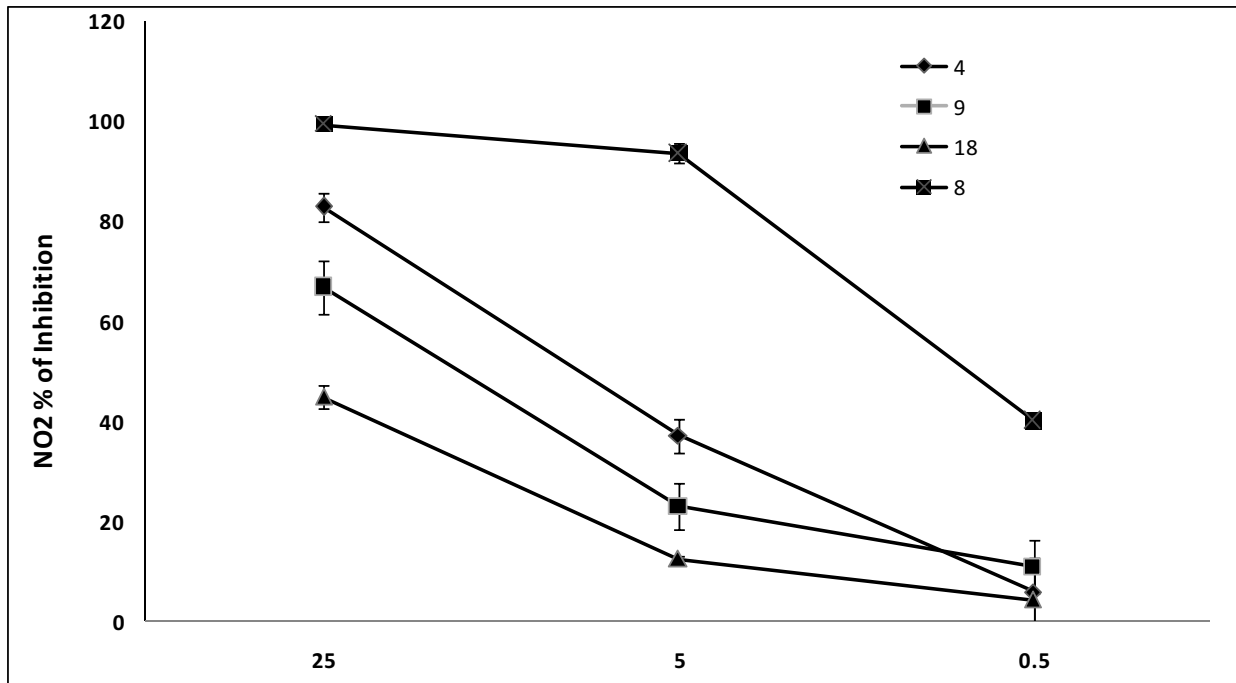


Figure-4:

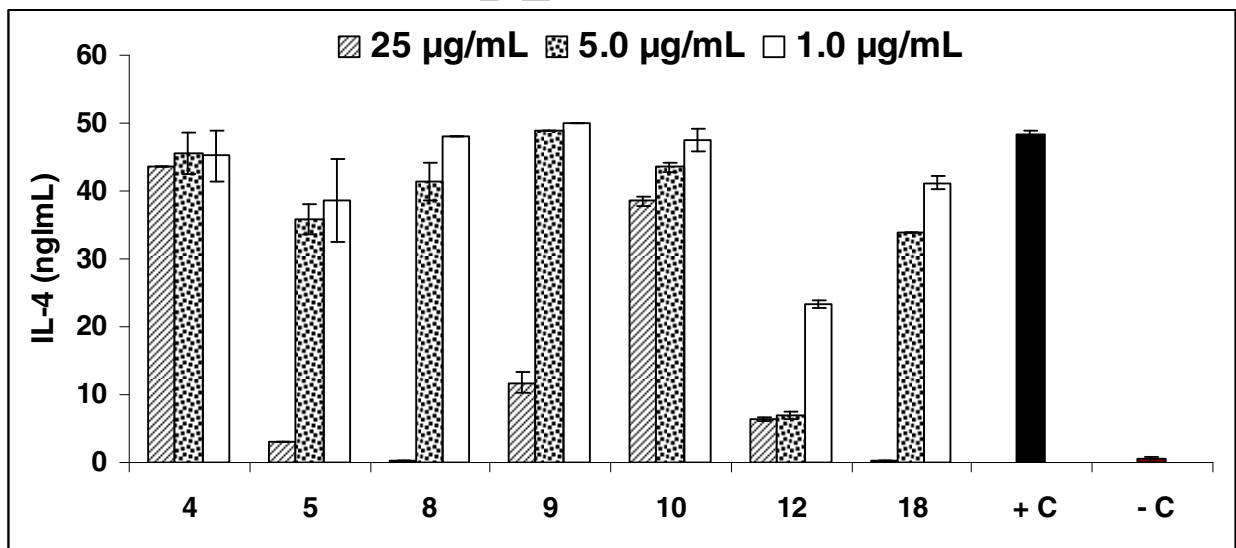
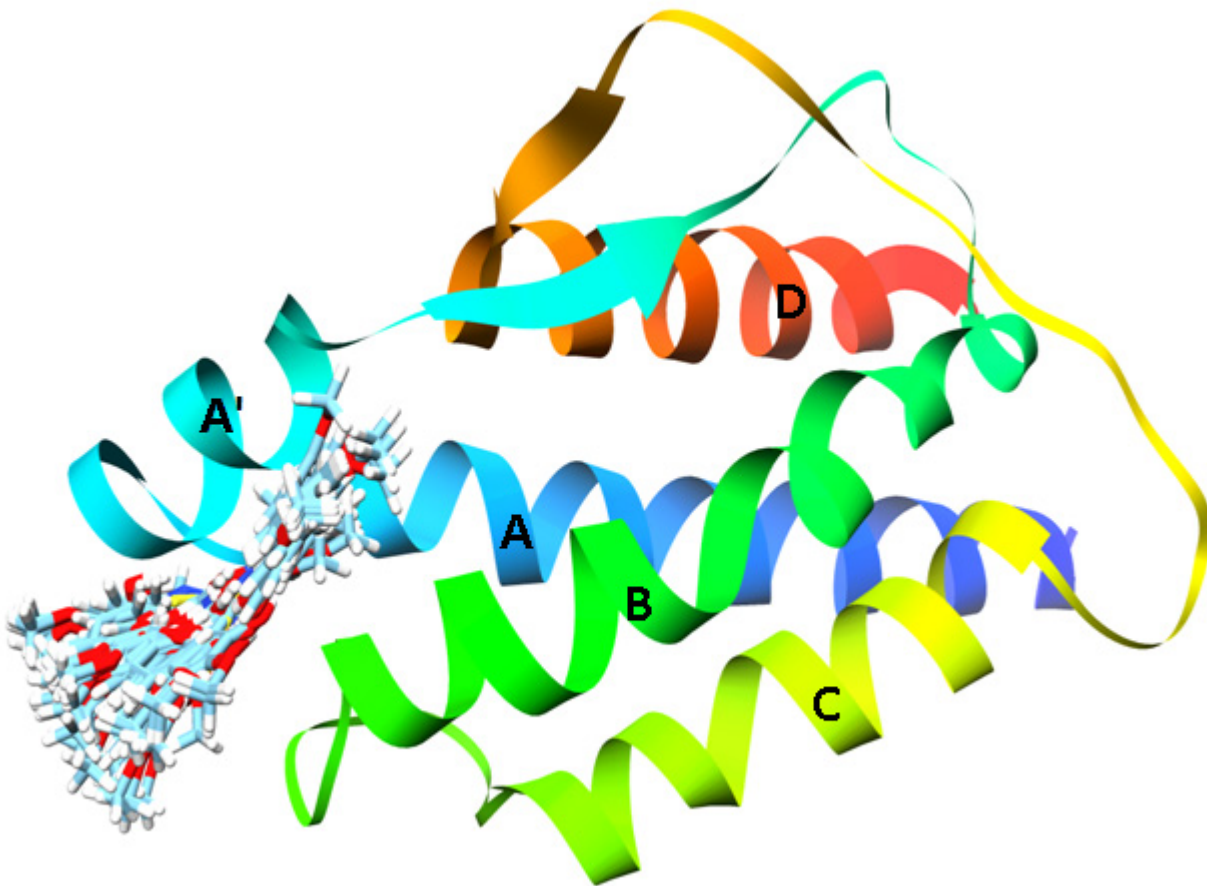
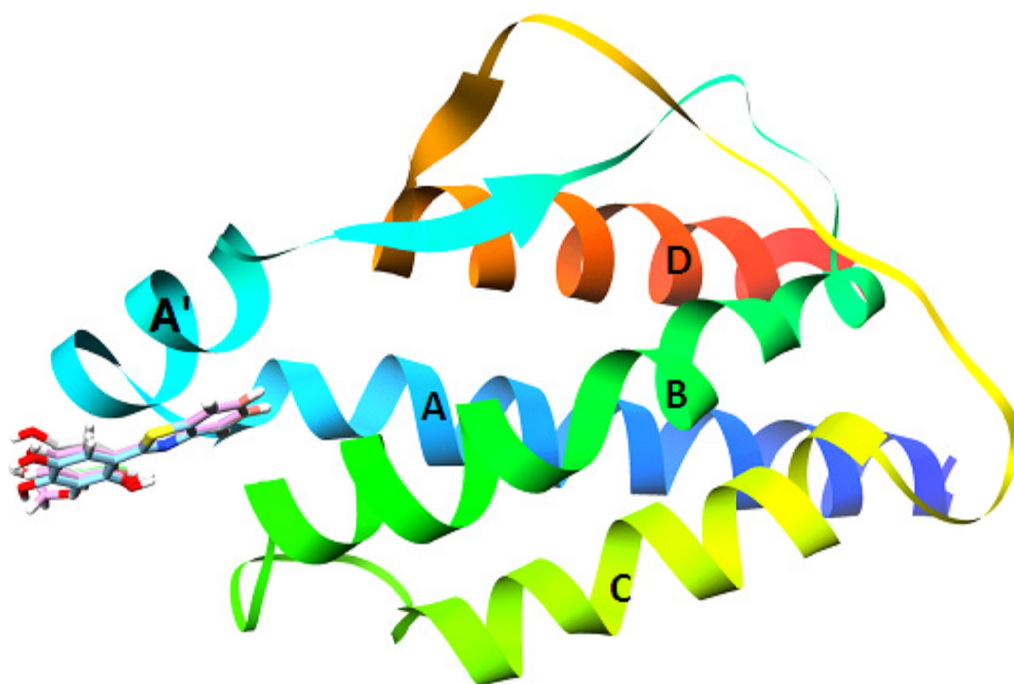


Figure-5a:



ACCEPTED

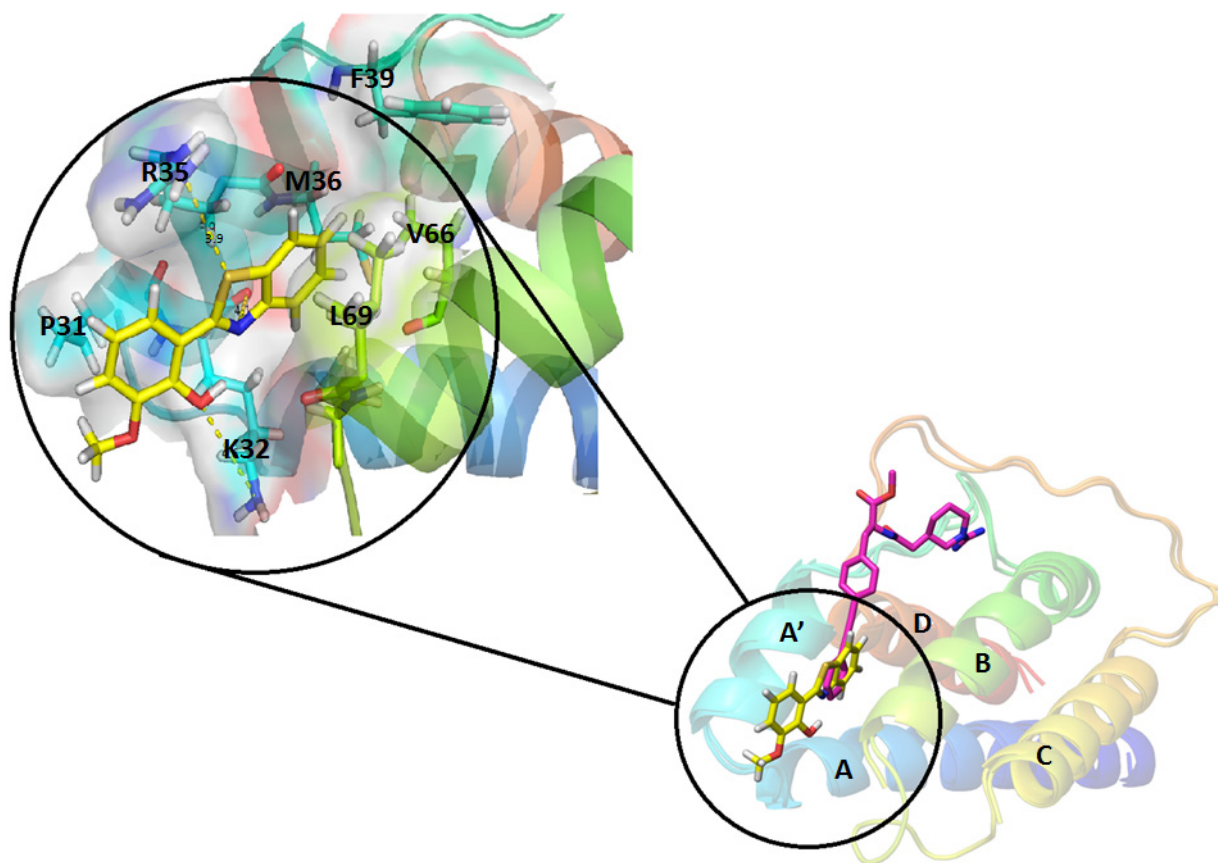
Figure-5b:



ACCEPTED MANUSCRIPT

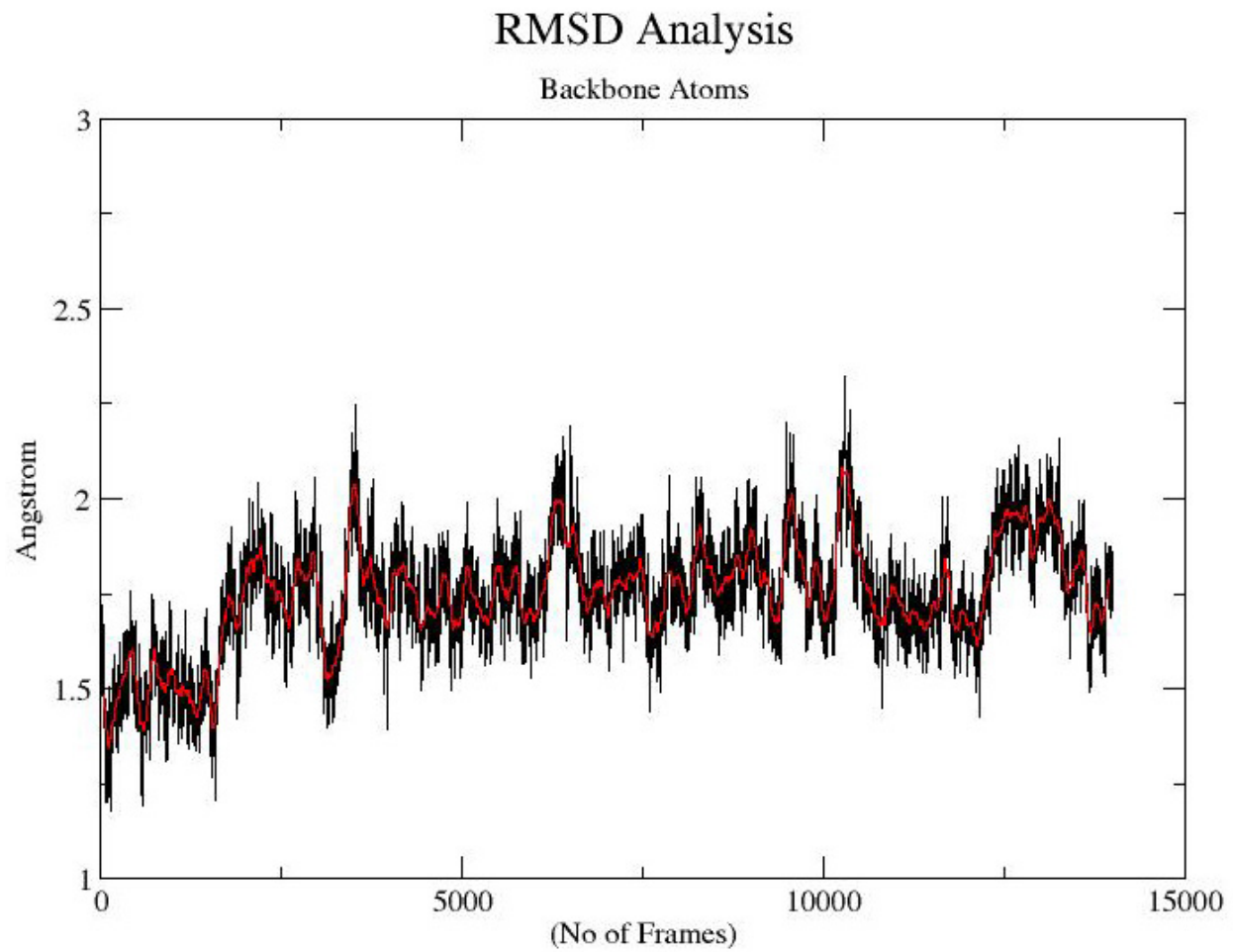
RIPT

Figure-5c:

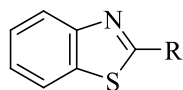


ACCEPTED

Figure-6:



ACCEPT



Basic Skeleton of Benzothiazole

Table-1: Structure of the Benzothiazoles (1-26) that were evaluated for anti-inflammatory activity

Comp. No.	R	Comp. No.	R	Comp. No.	R
1		10		19	
2		11		20	
3		12		21	
4		13		22	
5		14		23	
6		15		24	
7		16		25	

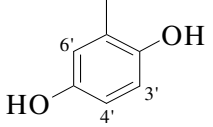
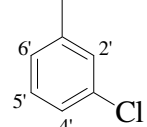
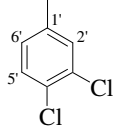
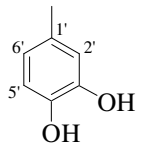
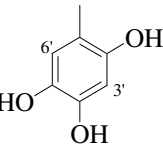
8		17		26	
9		18			

Table-2: Effect of benzothiazoles (1-26) on phagocyte oxidative burst activity and nitrite production

Compounds	IC ₅₀ (μg/mL) for phagocytes ROS	% of NO inhibited by 25 μg/mL of compounds	Cytotoxicity IC ₅₀ (μg/mL)
1	>100	26.5 ± 0.0	ND
2	1.9 ± 0.6	28.9 ± 1.3	>25
3	>100	20.5 ± 5.9	ND
4	>100	56.1 ± 0.6	>25
5	>100	44.5 ± 0.3	>20
6	34.3 ± 4.4	35.5 ± 7.4	ND
7	>100	5.4 ± 2.8	ND
8	<1	91.1 ± 0.7	>20
9	3.7 ± 0.2	58.5 ± 3.3	11.4±1.8
10	1.1 ± 0.1	14.3 ± 1.0	ND
11	>100	-7.4 ± 3.0	ND
12	>100	-1.5 ± 0.6	ND
13	11.1 ± 0.9	32.7 ± 8.3	11.5±0.0
14	11.8 ± 1.2	16.8 ± 0.8	>25
15	>100	10.8 ± 2.4	ND
16	>100	20.2 ± 1.5	ND
17	81.0 ± 4.1	14.1 ± 3.0	ND
18	>100	78.1 ± 1.6	10.4±1.3
19	>100	11.7 ± 1.7	ND
20	15.5 ± 1.0	41.6 ± 4.7	>25
21	>100	11.5 ± 2.7	ND

22	>100	23.5 ± 3.7	ND
23	>100	28.4 ± 2.5	ND
24	14.4 ± 2.5	30.3 ± 0.3	>25
25	>100	20.6 ± 5.3	ND
26	>100	35.7 ± 1.5	ND

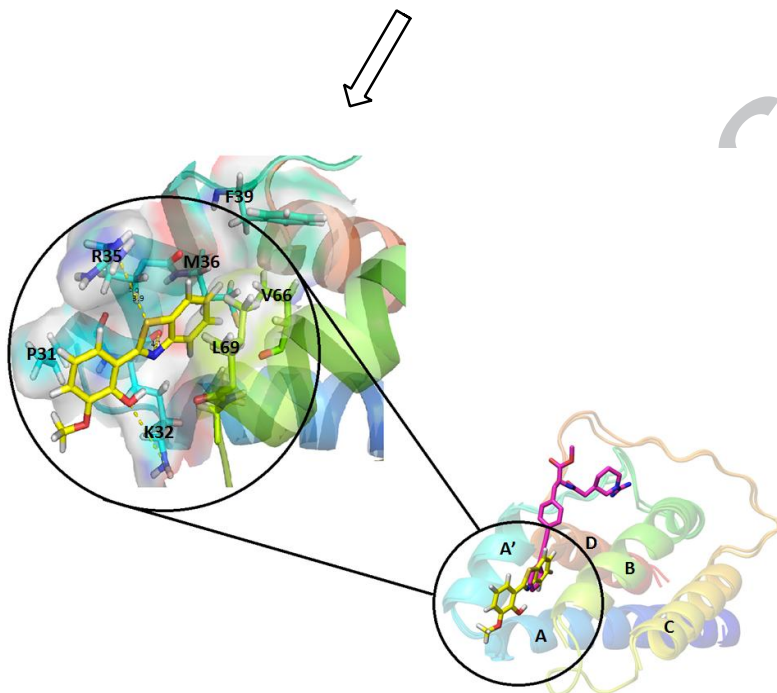
Generation of Reactive Oxygen Species (ROS), produced by human blood phagocytes, and Nitric Oxide (NO), produced by mice macrophages J774.2 cell line, were determined as described in the Material and Methods section. Results are presented as means ± SD of triplicate measurements. ND = not determined; control 1 = ibuprofen, control 2 = N^G-monomethyl-L-arginine, control 3 = cyclohexamide

Table-3: GOLD-Predicted Docking Scores of Compounds **2**, **8**, **18**, **4**, and **5**

S. No.	Compounds	IC ₅₀ in μ M for IL-2 production	GOLD Score
1	2	< 4.0	45.82
2	8	< 4.0	45.81
3	18	4.2 ± 0.4	44.42
4	4	12.8 ± 3.1	43.40
5	5	26 ± 3.5	42.15

Graphical abstract

Compound **2**, **4**, **8** and **18** the potent IL-2 inhibitors

**Highlights:**

- Benzothiazole Derivatives were synthesized
- Effects in Immune System Disorders (*in vitro studies*) were evaluated.
- New Immunomodulatory Agents were identified
- Structure-activity Relationship was established
- *In silico* Studies were performed